Research in Pharmaceutical Sciences, June 2025; 20(3): 343-355
Received: 06-03-2024
Peer Reviewed: 05-05-2024
Revised: 11-06-2024
Accepted: 16-06-2024
Published: 17-06-2025

School of Pharmacy & Pharmaceutical Sciences
Isfahan University of Medical Sciences

Original Article

Klotho microinjection into the RVLM attenuates acute kidney injury *via* interaction with the cholinergic anti-inflammatory pathway in rats

Fatemeh Ahmadi[1], Elahe Amohashemi[1], Mohammad Kazemi[2], Hossein Salehi[3], and Parham Reisi[1,4,*]

[1]*Department of Physiology, School of Medicine, Isfahan University of Medical Sciences, Isfahan, I.R. Iran.*
[2]*Department of Genetics and Molecular Biology, School of Medicine, Isfahan University of Medical Sciences, Isfahan, I.R. Iran.*
[3]*Department of Anatomical Sciences, School of Medicine, Isfahan University of Medical Sciences, Isfahan, I.R. Iran.*
[4]*Applied Physiology Research Center, Cardiovascular Research Institute, Isfahan University of Medical Sciences, Isfahan, I.R. Iran.*

Abstract

Background and purpose: The Klotho (*Klo*) gene, an aging suppressor in rats, accelerates aging when disrupted and extends lifespan when overexpressed. It encodes a transmembrane protein primarily expressed in renal tubules. This study investigated the protective effects of central Klo, both alone and in combination with cholinergic anti-inflammatory pathway (CAP) inhibition, against ischemia-reperfusion injury (IRI)-induced acute kidney injury. The current study evaluated the expression of inflammatory and anti-inflammatory genes (including *Il1b, Tnfa, Tgfb, Trem2,* and *Il10*) in the kidney, alongside plasma levels of creatinine (Cr), blood urea nitrogen (BUN), and signs of acute tubular injury.
Experimental approach: Klo was microinjected into the rostral ventrolateral medulla, and CAP inhibition was achieved through intraperitoneal administration of mecamylamine (Mec). Real-time RT-PCR and hematoxylin and eosin staining were used for gene expression analysis and histopathological examination, respectively.
Findings/Results: The results showed elevated Cr and BUN levels, tubular injury, and increased inflammatory gene expression in IRI and IRI + Mec groups, as well as reduced *Il10* in the IRI + Mec group. Klo exhibited protective effects. Elevated *Tgfb* expression was seen in IRI + Klo and IRI + Mec + Klo groups one week post-surgery.
Conclusion and implications: These findings indicated Klo potential to extend lifespan and protect against age-related diseases, including kidney disease and inflammation, *via* neural modulation of peripheral immunity.

Keywords: Acute kidney injury; Cholinergic anti-inflammatory pathway; Klotho; Mecamylamine; Rostral ventrolateral medulla.

INTRODUCTION

Klotho (Klo), an activator of fibroblast growth factor 23 (1), reduces tumor necrosis factor-α (TNF-α) and transforming growth factor-β (TGF-β) levels (2,3). It exists in 3 subfamilies, including α-Klo, β-Klo, and γ-Klo, with receptors identified in the brain, including the medulla (4). Klo, known for its interaction with erythropoietin as a protective factor (5) and anti-aging properties (6), influences brain processes such as learning and memory (7). However, Klo, highly concentrated in the kidney distal convoluted tubules (8) and the brain choroid plexus (9), is crucial for erythropoietin production and the metabolism of calcium, phosphate, and vitamin D (5,10).

*Corresponding author: P. Reisi
Tel: +98-3137929033, Fax: +98-3136688597
Email: parhamzh@gmail.com, p_reisi@med.mui.ac.ir

Access this article online	
	Website: http://rps.mui.ac.ir
	DOI: 10.4103/RPS.RPS_46_24

Enhanced Klo expression *via* genetic manipulation improves kidney function and morphology in chronic and acute kidney injuries (AKI) (11). Klo deficiency, an early event in AKI (12), exacerbates inflammatory cytokines (12,13)potentially worsening kidney function, glomerulonephritis, and chronic kidney disease (14,15). The conditions are further complicated by infection-triggered renal inflammation, ischemia-reperfusion injury (IRI), and immune complex deposition (16).

The cholinergic anti-inflammatory pathway (CAP) facilitates cross-talk between the immune and nervous systems, impacting both innate and adaptive immunities (17). The α7-nicotinic acetylcholine receptors (nAChRs) are crucial mediators of the interactions (18).

Klo, found as a neuropeptide in the rostral ventrolateral medulla (RVLM), reduces neuron activity (4) and regulates postganglionic sympathetic fibers to organs such as the kidneys (19). The fibers affect immune cells and inflammatory cytokines (20). The RVLM also integrates higher center information for blood pressure regulation, coordinating sympathetic output (21).

This study specifically aimed to assess the protective role of Klo against peripheral inflammations. Accordingly, we administered an extremely low dose of Klo in the medulla, insufficient to directly exhibit antioxidant effects on peripheral tissues. Instead, we focused on evaluating the neuropeptide-like action of Klo on anti-inflammatory pathways regulated by the autonomic nervous system. Additionally, the peripheral secondary effects of Klo were explored by examining its influence on the control centers of the autonomic nervous system. The current findings provided valuable insights into the role of the CAP system and the indirect protective function of the sympathetic system.

MATERIALS AND METHODS

Animals

This study employed an experimental design using male Wistar albino rats (weighing 200-250 g) obtained from the animal house of the School of Pharmacy and Pharmaceutical Sciences (Isfahan, Iran). The rats were maintained under a 12-h light-dark cycle with unlimited access to food and water. Each rat was housed individually in a polypropylene cage with wood shavings replaced with new ones daily. The cages were numerically designated, and each rat was randomly assigned to a cage. This study was approved by the Ethics Committee of the Isfahan University of Medical Sciences with ethical code IR.MUI.MED.REC.1400.626. In addition, all experimental procedures were conducted in accordance with the National Institute of Health Guide for the Care and Use of Laboratory Animals (NIH Publications No. 80-23), revised 2010.

Experimental design

Eighty rats were randomly divided into 8 groups (n = 10). Group 1 was exposed by surgery procedure without inducing IRI accompanied by intraperitoneal (IP) injection of saline as mecamylamine (Mec) vehicle and injection of saline as Klo vehicle into RVLM (sham); group 2 was exposed by surgery procedure without inducing IRI accompanied by IP injection of Mec and injection of Klo vehicle into RVLM (sham + Mec); group 3 was exposed by surgery procedure without inducing IRI accompanied by IP injection of Mec vehicle and injection of Klo into RVLM (sham + Klo); group 4 was exposed by surgery procedure without inducing IRI accompanied by IP injection of Mec and injection of Klo into RVLM (sham + Mec + Klo); group 5 was exposed by IRI accompanied by IP injection of Mec vehicle and injection of Klo vehicle into RVLM (IRI); group 6 was exposed by IRI accompanied by IP injection of Mec and injection of Klo vehicle into RVLM (IRI + Mec); group 7 was exposed by IRI accompanied by IP injection of Mec vehicle and injection of Klo into RVLM (IRI + Klo); group 8 was exposed by IRI accompanied by IP injection of Mec and injection of Klo into RVLM (IRI + Mec + Klo). Twenty-four h and 7 days post-treatment, 3 rats from each group at each time point were selected for gene expression analysis. Additionally, 7 days post-treatment, the remaining 4 rats were sacrificed for histological analysis. In all rats, body and

kidney weight measurements, as well as the assessment of serum blood urea nitrogen (BUN) and creatinine (Cr) levels, were conducted at different time points (22).

IRI surgical procedure

To induce IRI, rats were anesthetized with ketamine (100 mg/kg, IP) (23,24) and xylazine (5 mg/kg, IP) (25) followed by the administration of Mec (3 mg/kg, IP; Cat. No. FM32263, Biosynth Company, UK) (26) 10 min before IRI. After warming on a 37 °C heating pad, both right and left flanks were shaved, disinfected. Also, the eyes were covered with tetracycline ointment to prevent dryness and damage. A 3-cm dorsal incision in each flank exposed the kidneys. After that, the arteries and veins on both sides were clamped for 60 min (27), indicated by a dark red hue. Reperfusion started once the kidneys regained their original color. Then, rats received 0.9% saline solution (1 mL; IP) for hydration, and the incisions were closed. Post-surgery, the animals were treated with tetracycline ointment to cover the wound and prevent infection, and morphine (5 mg/kg; IP) was administered for analgesia, with free access to food and water. Sham groups underwent a similar surgical process without renal pedicle closure.

Stereotaxic surgical procedure

During the initial 30 min of ischemia, the head of the animals was fixed in a stereotaxic apparatus (Stoelting, USA). A cannula was inserted into the RVLM on the right side of the brain, using coordinates from Paxinos and Watson's atlas (28) (2.4 mm lateral, -12.3-12.4 mm posterior, and 9.9 mm deep to the bregma) (Fig. 1). Klo (0.15 µg/rat; Cat. No. APH757Ra01, Cloud-Clone Corp Co., USA) was then microinjected into the RVLM. The Klo dosage was calculated based on studies involving brain ventricle injections in rodents and *in vitro* RVLM research, considering brain nuclei size and volume (29-33). Animals were included in the study if both IRI and microinjection were successfully performed. Excremental time was between 09.30 am to 12.30 pm, and each animal was examined at a different time each day.

Measurement of biochemical parameters

On the 7th day, the rats were deeply anesthetized with urethane (1.6 g/kg; IP), and blood samples were taken through cardiac puncture. Blood samples were centrifuged to separate serum (5000 rpm for 10 min). Cr and BUN concentrations were measured with an auto-analyzer (SRL, Tokyo, Japan) as indicators of renal dysfunction.

Histopathological examination

After decapitation, the right kidney was removed from 4 rats in each experimental group. Renal samples were fixed in 10% formalin for 24 h. Paraffin wax tissue blocks were cut to obtain 4 µm-thick sections. After collecting the renal sections on a glass slide and deparaffinizing, they were stained with hematoxylin and eosin to be examined under a light microscope. Different renal sections were evaluated histologically by 2 blinded pathologists who scored the sections with a specific scale to assess the degree of renal tubule interstitial damage. The kidney scoring system, including 0 (< 5%), 1 (5-20%), 2 (20-50%), 3 (50-70%), and 4 (< 70%), was used. At least 10 fields (200× magnification) were examined for each kidney section and assigned for renal injury (Table 1).

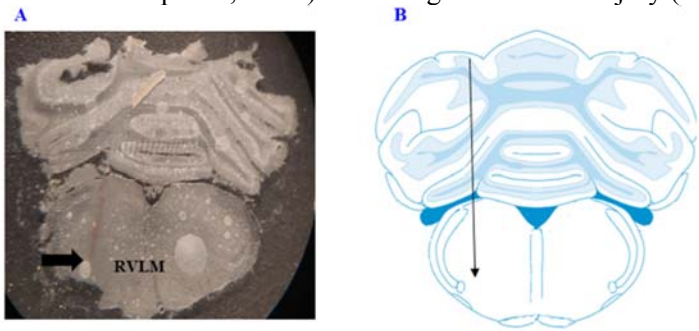

Fig. 1. (A) Coronal photomicrograph of injection site in the RVLM and (B) a representative image, displaying the microinjection site in the RVLM. RVLM, Rostral ventrolateral medulla.

Table 1. Evaluation of degree of renal tubule interstitial damage.

Histopathological changes	0 (< 5%)	1 (5-20%)	2 (< 20-50%)	3 (< 50-70%)	4 (> 70%)
Tubular vacuolization					
Tubular dilatation					
Tubular cast formation					
Loss of brush border					
Desquamation					
Necrotic tubules					

Table 2. Primer sequences used in real-time PCR experiments.

Gene name	Primer sequence (5′ to 3′)	Accession No.	Amplicon size (bp)
Gapdh	Forward: GGCAAGTTCAACGGCACAG	NM_017008.4	142
Gapdh	Reverse: CGCCAGTAGACTCCACGACAT		
Il1b	Forward: GGCTTCCTTGTGCAAGTGTCTGA	NM_031512.2	199
Il1b	Reverse: CGAGATGCTGCTGTGAGATTTGAA		
Il10	Forward: CCCAGAAATCAAGGAGCATT	NM_012854.2	129
Il10	Reverse: TCATTCTTCACCTGCTCCAC		
Tgfb	Forward: TGAACCAAGGAGACGGAATACA	NM_021578.2	163
Tgfb	Reverse: GCCATGAGGAGCAGGAAGG		
Tnf	Forward: CGCTCTTCTGTCTACTGAACTT	NM_012675.3	166
Tnf	Reverse: GCTTGGTGGTTTGCTACGA		
Trem2	Forward: TTCTTACAGCCAGCATCCT	NM_001106884.1	155
Trem2	Reverse: CTCCTCCTACTCAGACTTCTC		

Real-time RT-PCR technique

The research objective was to determine the expression of inflammatory and anti-inflammatory genes in 3 rats from each experimental group through the removal of the right kidney. The FavorPrep™ Tissue Total RNA Mini Kit (Favorgen, Taiwan) was employed to isolate total RNA from the tissue, as per the manufacturer's guidelines. The quantity and quality of the isolated RNA were measured by assessing its absorbance at 260 nm and 280 nm using a NanoDropTM 2000 (Thermo Fisher Scientific, USA). One µg of total RNA was utilized for cDNA synthesis, utilizing the easy cDNA reverse transcription kit (ParsTous, Iran) and oligo dT primers. Real-time PCR was executed using RealQ Plus 2× Master Mix Green (Ampliqon, Denmark) and the StepOnePlus™ real-time PCR detection system (Applied Biosystems). Specific gene primers were created by using AlleleID V7.8 software (available at http://premierbiosoft.com), and their sequences are shown in Table 2. The PCR amplification conditions consisted of a 15-min denaturation step at 95 °C, followed by 40 cycles with a 20-s denaturation at 95 °C, and then annealing and extending for 1 min at 60 °C. Melting curve analysis was conducted to determine the melting temperature of both specific amplification products and primers. The experiments were performed in triplicate and independently repeated at least 3 times. To determine the expression level of each target gene, glyceraldehyde-3-phosphate dehydrogenase was used as an endogenous control and calculated as $2^{-\Delta\Delta Ct}$ according to previously described methods (34).

Statistical analysis

Data were expressed as mean ± SEM and analyzed using SPSS version 21 for Windows. Statistical analysis was performed using univariate ANOVA to assess between-subjects effects, including the effects of IRI, Mec, Klo, and their interactions. Additionally, one-way ANOVA followed by Tukey post hoc test, as well as unpaired t-tests, were conducted to compare the groups (the results of these analyses were presented in the Figurs). A level of $P < 0.05$ was considered statistically significant.

RESULTS

Effects of intra-RVLM microinjection of Klo alone or in combination with CAP inhibition on BUN levels following AKI

One day after IRI, a significant increase was observed in the BUN level in the IRI rats compared to sham rats (IRI effect, F (1,16) = 204.948, $P < 0.001$; Fig. 2A). Mec enhanced the BUN level compared to vehicle-treated rats (Mec effect, F (1,16) = 10.352, $P = 0.005$; Fig. 2A). Also, Klo reduced the BUN level compared to vehicle-treated rats (Klo effect, F (1,16) = 13.698, $P = 0.002$; Fig. 2A). Mec raised the BUN level in IRI rats (IRI × Mec interaction effect, F (1,16) = 7.459, $P = 0.015$; Fig. 2A). Klo alleviated the BUN level in IRI rats (IRI × Klo interaction effect, F (1,24) = 13.692, $P = 0.002$; Fig. 2A). Other interactions did not have significant changes on the BUN level. In the measurement of BUN during 7 days after IRI, the effects and interactions did not show significant changes in the BUN level.

Effects of intra-RVLM microinjection of Klo alone or in combination with CAP inhibition on Cr levels following AKI

One day after IRI, a significant elevation was observed in the Cr level in the IRI rats compared to sham rats (IRI effect, F (1,16) = 33.503, $P < 0.001$; Fig. 2B). Mec augmented the Cr level compared to vehicle-treated rats (Mec effect, F (1,16) = 4.358, $P = 0.053$; Fig. 2B). Mec enhanced the Cr level in IRI rats (IRI × Mec interaction effect, F (1,16) = 4.729, $P = 0.045$; Fig. 2B). Other effects and interactions did not have significant changes on the Cr level. In the measurement of Cr during 7 days after IRI, all effects and interactions did not show significant changes in the Cr level.

Effects of intra-RVLM microinjection of Klo alone or in combination with CAP inhibition on the kidney expression of interleukin 1 β gene following AKI

One day after IRI, a significant upregulation in interleukin 1 β (*Il1b*) gene expression was observed in the IRI rats compared to sham rats (IRI effect, F (1,16) = 9.672, $P = 0.007$; Fig. 3A). Klo downregulated *Il1b* gene expression compared to vehicle-treated rats (Klo effect, F (1,16) = 5.582, $P = 0.031$; Fig. 3A). Other effects and interactions did not show significant changes in *Il1b* gene expression in the kidney.

Seven days after IRI, a significant increase in *Il1b* gene expression was observed in the IRI rats compared to sham rats (IRI effect, F (1,17) = 752.162, $P < 0.001$; Fig. 3A). Mec augmented *Il1b* gene expression compared to vehicle-treated rats (Mec effect, F (1,17) = 68.338, $P < 0.001$; Fig. 3A). Also, Klo alleviated *Il1b* gene expression compared to vehicle-treated rats (Klo effect, F (1,17) = 148.905, $P < 0.001$; Fig. 3A). Klo suppressed *Il1b* gene expression in IRI rats (IRI × Klo interaction effect, F (1,17) = 50.571, $P < 0.001$; Fig. 3A). Other interactions did not have significant changes in *Il1b* gene expression in the kidney.

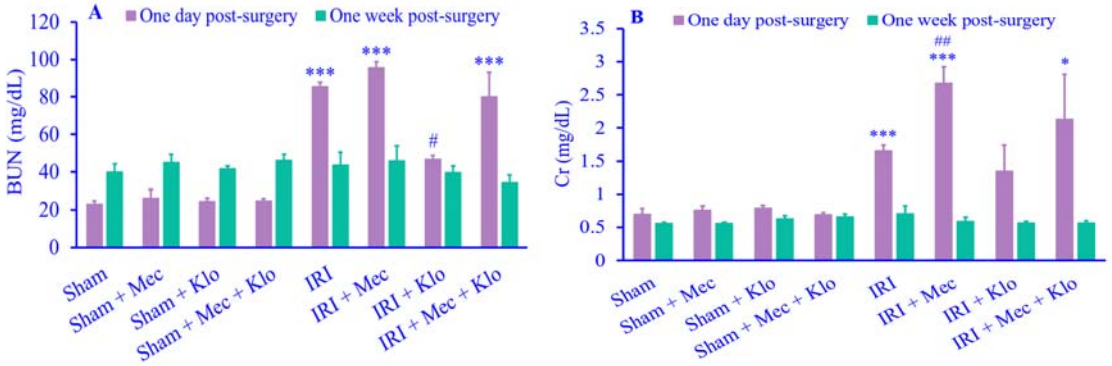

Fig. 2. Effects of intra-rostral ventrolateral medulla microinjection of Klo alone or in combination with cholinergic anti-inflammatory pathway inhibition on the levels of (A) BUN and (B) Cr at 24 h (n = 3) and one week post-surgery (n = 7) following acute kidney injury in rats. Animals received Mec at the dose of 3 mg/kg, intraperitoneally. Klo was injected (0.15 µg/rat) into the RVLM. Sham groups underwent a surgical process without renal pedicle closure. Data were expressed as mean ± SEM. $^{*}P < 0.05$ and $^{***}P < 0.001$ indicate significant differences when compared with respective sham group; $^{\#}P < 0.05$ and $^{\#\#}P < 0.$ 01 versus respective IRI group. Mec, Mecamylamine; Klo, Klotho; IRI, ischemia-reperfusion injury; BUN, blood urea nitrogen; Cr, creatinine.

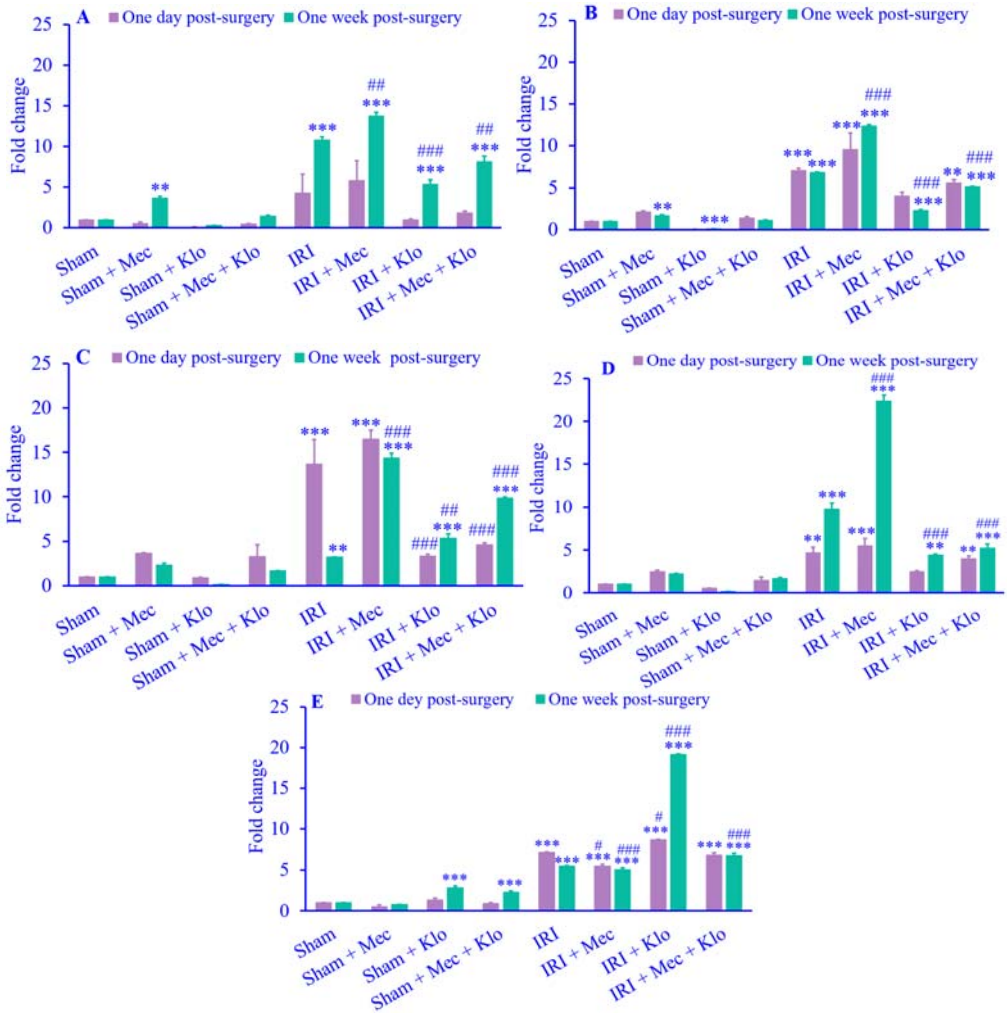

Fig. 3. Effects of intra-rostral ventrolateral medulla microinjection of Klo alone or in combination with cholinergic anti-inflammatory pathway inhibition on the kidney expression of (A) interleukin 1 β, (B) tumor necrosis factor α, (C) transforming growth factor β, (D) triggering receptor myeloid cells 2, and (E) interleukin 10 genes at 24 h and one week post-surgery following acute kidney injury in rats. Animals received Mec at the dose of 3 mg/kg, intraperitoneally. Klo (0.15 µg/rat) was injected into the RVLM. Sham groups underwent a surgical process without renal pedicle closure. Data were expressed as mean ± SEM, n = 3. $^{**}P < 0.01$, and $^{***}P < 0.001$ indicate significant differences when compared with the respective sham group; $^{\#}P<0.05$, $^{\#\#}P<0.01$, and $^{\#\#\#}P<0.001$ versus respective IRI group. Mec, Mecamylamine; Klo, Klotho; IRI, ischemia-reperfusion injury.

Effects of intra-RVLM microinjection of Klo alone or in combination with CAP inhibition on the kidney expression of Tnfa gene following AKI

One day after IRI, a significant boost in *Tnfa* gene expression was observed in the IRI rats compared to sham rats (IRI effect, F(1,16) = 105.371, $P < 0.001$; Fig. 3B). Mec upregulated *Tnfa* gene expression compared to vehicle-treated rats (Mec effect, F (1,16) = 9.667, $P = 0.007$; Fig. 3B). Also, Klo reduced *Tnfa* gene expression compared to vehicle-treated rats (Klo effect, F (1,16) = 16.749, $P = 0.001$; Fig. 3B). Klo inhibited T*nfa* gene expression in IRI rats (IRI × Klo interaction effect, F (1,16) = 6.209, $P = 0.024$; Fig. 3B). Other interactions did not have significant changes in T*nfa* gene expression in the kidney.

One week after IRI, a significant rise in T*nfa* gene expression was observed in the IRI rats compared to sham rats (IRI effect, F(1,17) = 7552.276, $P < 0.001$; Fig. 3B). Mec upregulated T*nfa* gene expression compared to vehicle-treated rats (Mec effect, F (1,17) = 1509.819, $P < 0.001$; Fig. 3B). Also, Klo blocked T*nfa* gene expression compared to vehicle-treated rats (Klo effect, F (1,17) = 2505.546, $P < 0.001$; Fig. 3B). Mec increased T*nfa* gene expression in IRI rats (IRI × Mec interaction effect, F (1,17) = 672.755, $P < 0.001$; Fig. 3B). Klo

downregulated T*nfa* gene expression in IRI rats (IRI × Klo interaction effect, F (1,17) = 1519.267, $P < 0.001$; Fig. 3B) and Mec-treated rats (Mec × Klo interaction effect, F (1,17) = 82.240, $P < 0.001$; Fig. 3B). Concurrent interactions among 3 interventions suppressed T*nfa* gene expression (IRI × Mec × Klo interaction effect, F (1,17) = 139.352, $P < 0.001$; Fig. 3B).

Effects of intra-RVLM microinjection of Klo alone or in combination with CAP inhibition on the kidney expression of Tgfb gene following AKI

One day after IRI, a significant escalation in *Tgfb* gene expression was observed in the IRI rats compared to sham rats (IRI effect, F (1,16) = 81.253, $P < 0.001$; Fig. 3C). Mec upregulated *Tgfb* gene expression compared to vehicle-treated rats (Mec effect, F (1,16) = 7.907, $P = 0.013$; Fig. 3C). Also, Klo suppressed *Tgfb* gene expression compared to vehicle-treated rats (Klo effect, F (1,16) = 48.963, $P < 0.001$; Fig. 3C). Klo decreased *Tgfb* gene expression in IRI rats (IRI × Klo interaction effect, F (1,16) = 44.866, $P < 0.001$; Fig. 3C). Other interactions did not have significant changes in *Tgfb* gene expression in the kidney.

Seven days after IRI, a significant elevation in *Tgfb* gene expression was observed in the IRI rats compared to sham rats (IRI effect, F (1,17) = 974.254, $P < 0.001$; Fig. 3C). Mec increased *Tgfb* gene expression compared to vehicle-treated rats (Mec effect, F (1,17) = 437.098, $P < 0.001$; Fig. 3C). Also, Klo downregulated *Tgfb* gene expression compared to vehicle-treated rats (Klo effect, F (1,17) = 19.595, $P < 0.001$; Fig. 3C). Mec enhanced *Tgfb* gene expression in IRI rats (IRI × Mec interaction effect, F (1,17) = 208.634, $P < 0.001$; Fig. 3C). Mec-treated rats diminished *Tgfb* gene expression (Mec × Klo interaction effect, F (1,17) = 53.039, $P < 0.001$; Fig. 3C). Concurrent interactions among 3 interventions raised *Tgfb* gene expression (IRI × Mec × Klo interaction effect, F (1,17) = 58.998, $P < 0.001$; Fig. 3C).

Effects of intra-RVLM microinjection of Klo alone or in combination with CAP inhibition on the kidney expression of triggering receptor myeloid cells 2 gene following AKI

One day after IRI, a significant increase in triggering receptor myeloid cells 2 (*Trem2)* gene expression was observed in the IRI rats compared to sham rats (IRI effect, F (1,16) = 68.933, $P < 0.001$; Fig. 3D). Mec boosted *Trem2* gene expression compared to vehicle-treated rats (Mec effect, F (1,16) = 12.728, $P = 0.003$; Fig. 3D). Also, Klo declined *Trem2* gene expression compared to vehicle-treated rats (Klo effect, F (1,16) = 14.877, $P = 0.001$; Fig. 3D). The interactions did not have significant changes in *Trem2* gene expression in the kidney.

One week after IRI, a significant increment in *Trem2* gene expression was observed in the IRI rats compared to sham rats (IRI effect, F (1,17) = 782.332, $P < 0.001$; Fig. 3D). Mec upregulated *Trem2* gene expression compared to vehicle-treated rats (Mec effect, F (1,17) = 151.067, $P < 0.001$; Fig. 3D). Also, Klo attenuated *Trem2* gene expression compared to vehicle-treated rats (Klo effect, F (1,17) = 333.207, $P < 0.001$; Fig. 3D). Mec raised *Trem2* gene expression in IRI rats (IRI × Mec interaction effect, F (1,17) = 65.867, $P < 0.001$; Fig. 3D). Klo decreased *Trem2* gene expression in IRI rats (IRI × Klo interaction effect, F (1,17) = 259.359, $P < 0.001$; Fig. 3D) and Mec-treated rats (Mec × Klo interaction effect, F (1,17) = 76.219, $P < 0.001$; Fig. 3D). Concurrent interactions among 3 interventions reduced *Trem2* gene expression (IRI × Mec × Klo interaction effect, F (1,17) = 83.773, $P < 0.001$; Fig. 3D).

Effects of intra-RVLM microinjection of Klo alone or in combination with CAP inhibition on the kidney expression of interleukin 10 gene following AKI

One day after IRI, a significant enhancement in interleukin 10 (*Il10)* gene expression was observed in the IRI rats compared to sham rats (IRI effect, F (1,16) = 871.318, $P < 0.001$; Fig. 3E). Mec downregulated *Il10* gene expression compared to vehicle-treated rats (Mec effect, F (1,16) = 29.217, $P < 0.001$; Fig. 3E). Also, Klo upregulated *Il10* gene expression compared to vehicle-treated rats (Klo effect, F (1,16) = 18.307, $P = 0.001$; Fig. 3E). Mec suppressed *Il10* gene expression in IRI rats (IRI × Mec interaction effect, F (1,16) = 9.524, $P = 0.007$; Fig. 3E). Klo augmented *Il10* gene expression in IRI rats (IRI × Klo interaction effect, F (1,16) = 5.970, $P = 0.027$; Fig. 3E). Other interactions did not have significant changes in *Il10* gene expression in the kidney.

Seven days after IRI, a significant increase in *Il10* gene expression was observed in the IRI rats compared to sham rats (IRI effect, F (1,17) = 5195.217, $P < 0.001$; Fig. 3E). Mec inhibited *Il10* gene expression compared to vehicle-treated rats (Mec effect, F (1,17) = 1427.581, $P < 0.001$; Fig. 3E). Also, Klo upregulated *Il10* gene expression compared to vehicle-treated rats (Klo effect, F (1,17) = 992.921, $P < 0.001$; Fig. 3E). Mec declined *Il10* gene expression in IRI rats (IRI × Mec interaction effect, F (1,17) = 1197.930, $P < 0.001$; Fig. 3E). Klo improved *Il10* gene expression in IRI rats (IRI × Klo interaction effect, F (1,17) = 294.429, $P < 0.001$; Fig. 3E) and Mec-treated rats (Mec × Klo interaction effect, F (1,17) = 320.754, $P < 0.001$; Fig. 3E). Concurrent interactions among 3 interventions enhanced *Il10* gene expression (IRI × Mec × Klo interaction effect, F (1,17) = 22.402, $P < 0.001$; Fig. 3E).

Effects of intra-RVLM microinjection of Klo alone or in combination with CAP inhibition on acute tubular injury in the kidney

One week after IRI, as depicted in Fig. 4A and B, there was a significant increase in acute tubular injury in IRI rats compared to sham rats (IRI effect, F (1,24) = 803.141, $P < 0.001$; Fig. 4B). Mec increased acute tubular injury compared to vehicle-treated rats (Mec effect, F (1,24) = 238.261, $P < 0.001$; Fig. 4B). Also, Klo attenuated acute tubular injury compared to vehicle-treated rats (Klo effect, F (1,24) = 14.421, $P = 0.001$; Fig. 4B). Klo diminished acute tubular injury in IRI rats (IRI × Klo interaction effect, F (1,24) = 43.727, $P < 0.001$; Fig. 4B) and Mec-treated rats (Mec × Klo interaction effect, F (1,24) = 9.955, $P = 0.004$; Fig. 4B). Other interactions did not have significant changes in acute tubular injury in the kidney.

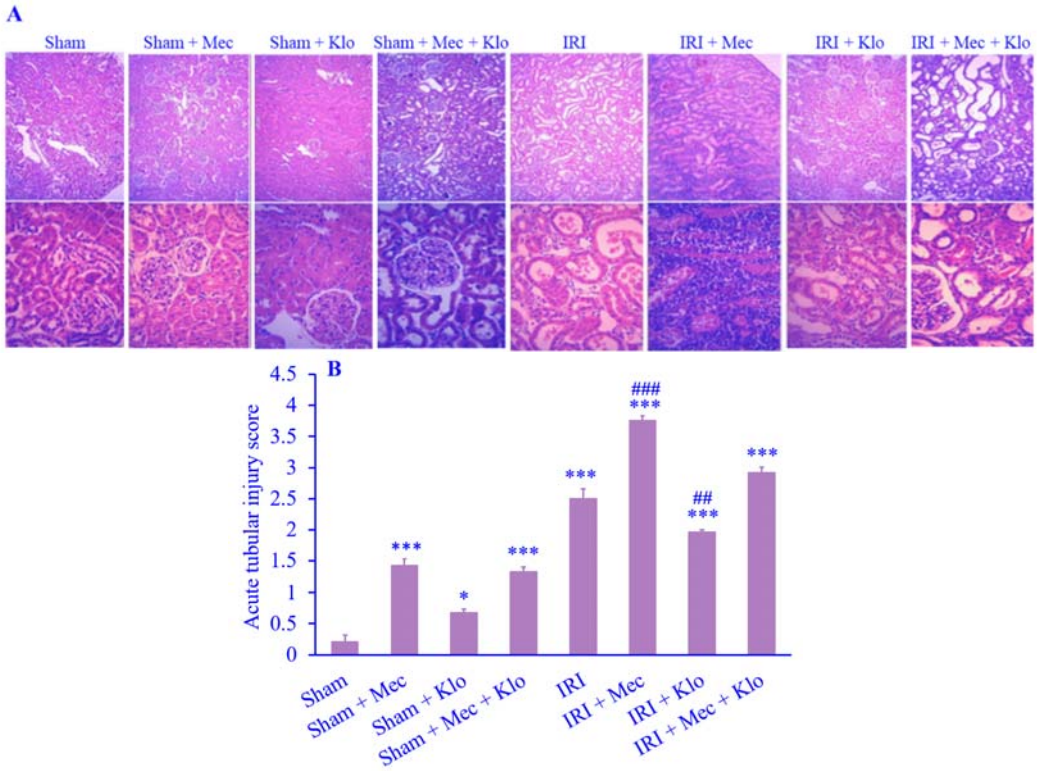

Fig. 4. Effects of intra-rostral ventrolateral medulla microinjection of Klo alone or in combination with cholinergic anti-inflammatory pathway inhibition on (A) histological changes in the kidney and (B) acute tubular injury score at one week post-surgery following acute kidney injury in rats. The first and second rows were magnified at 10× and 40×, respectively. Animals received Mec at the dose of 3 mg/kg, intraperitoneally. Klo was injected (0.15 µg/rat) into the RVLM. Sham groups underwent a surgical process without renal pedicle closure. Data were expressed as mean ± SEM, n = 4. $^{*}P < 0.05$ and $^{***}P < 0.001$ indicate significant differences when compared with respective sham group; $^{\#\#}P < 0.01$, and $^{\#\#\#}P < 0.001$ versus respective IRI group. Mec, Mecamylamine; Klo, Klotho; IRI, ischemia-reperfusion injury.

Fig. 5. Effects of intra-rostral ventrolateral medulla microinjection of Klo alone or in combination with cholinergic anti-inflammatory pathway inhibition on the percentage of (A) body weight change and (B) the kidney weight at 24 h (n = 3) and one week post-surgery (n = 7) following acute kidney injury in rats. Animals received Mec at the dose of 3 mg/kg, intraperitoneally. Klo was injected (0.15 µg/rat) into the RVLM. Sham groups underwent a surgical process without renal pedicle closure. Data were expressed as mean ± SEM. $^{*}P < 0.05$, $^{**}P < 0.01$, and $^{***}P < 0.001$ indicate significant differences when compared with the respective sham group; $^{\#}P < 0.05$ versus the respective IRI group. Mec, Mecamylamine; Klo, Klotho; IRI, ischemia-reperfusion injury.

Effects of intra-RVLM microinjection of Klo alone or in combination with CAP inhibition on percentage of body weight changes and kidney weight following AKI

One day after IRI, all effects and interactions did not show significant changes in the body weight of rats. One week after IRI, a significant reduction was observed in the body weight in the IRI rats compared to sham rats (IRI effect, F (1,48) = 15.838, $P < 0.001$; Fig. 5A). Klo decreased body weight of rats compared to vehicle-treated rats (Klo effect, F (1,48) = 6, $P < 0.05$; Fig. 5A). Concurrent interactions among 3 interventions suppressed body weight of rats (IRI × Mec × Klo interaction effect, F (1,48) = 10.665, $P < 0.01$; Fig. 5A).

One day after IRI, a significant boost was observed in the kidney weight in the IRI rats compared to sham rats (IRI effect, F (1,16) = 32.358, $P < 0.001$; Fig. 5B). Other effects and interactions did not have significant changes on the kidney weight. One week after IRI, a significant increase was observed in the kidney weight in the IRI rats compared to sham rats (IRI effect, F (1,24) = 15.795, $P = 0.001$; Fig. 5B). Other effects and interactions did not have significant changes on the kidney weight.

DISCUSSION

In this study, the primary aim was to evaluate the influence of Klo microinjection into the RVLM, with or without concurrent CAP inhibition, after IRI and the ensuing AKI, on the expression of anti-inflammatory gene *Il10*, alongside with inflammatory genes such as *Il1b*, *Tgfb*, *Tnfa*, and *Trem2* in the kidney. A single dose of Klo was administered directly into the RVLM. Although there was no specific reference for this exact dosage in the RVLM, this study relied on previous studies that used Klo injections into brain ventricles in rodents and *in vitro* studies on the RVLM. The dosage calculation considered brain nuclei size and volume, but it is essential to recognize that this approach has limitations (29-33). Additionally, to evaluate kidney function, the plasma levels of Cr and BUN were examined. Also, analyses were conducted on samples to quantify the extent of acute kidney damage, and the body and kidney weights were also measured. These evaluations were performed at both 24 h and one week following the surgery.

Histological assessments confirmed kidney damage in the experimental groups. On the first day post-surgery, groups with AKI-induced kidney ischemia showed elevated BUN and Cr levels, indicating severe damage. However, the IRI + Klo group exhibited significant tissue protection and a marked reduction in BUN levels. AKI, formerly known as acute renal failure, is characterized by a rapid decline in glomerular filtration rate (GFR) and the accumulation of waste products like BUN and Cr (35). Evidence links Klo levels to estimated GFR (36). Within a week, healthy nephrons in the IRI groups recovered normal function despite initial damage, resulting in BUN and Cr

levels comparable to the sham group. The sham groups, which did not experience direct kidney damage, maintained stable BUN and Cr levels. Interventions in the sham groups likely affected tissue through the autonomic system and peripheral controls rather than a direct kidney impact.

In all experimental groups, body weight decreased while kidney weight increased. Mec and IRI significantly enhanced the expression of inflammatory genes. During AKI, similar to other stressor conditions, inflammatory cytokines like Il1b and TNF-α are produced by activated innate immune cells (37,38). In Klo-treated groups, *Tgf-b* gene expression increased one week after IRI. Ischemic injury may release mediators such as angiotensin II and *Tgfb*, potentially reducing the expression of the endogenous anti-aging protein Klo (39). The decrease in *Klo* expression contributes to the aggravation of renal fibrosis by increasing the expression of *Tgfb*. Klo may bind directly to *Tgfb* receptors and prevent *Tgf-b* from binding to cell surface receptors. This mechanism disrupts *Tgfb* signaling, thereby abolishing the fibrogenic effects associated with *Tgfb* (2). Klo also induced an upregulation in the expression of *the Il10* gene. *Il10* is known to be an inhibitor of several inflammatory cytokines, including *Tnfa* (40).

Klo appears to modulate both inflammatory and anti-inflammatory gene levels in the kidney through various pathways. The brainstem and hypothalamus, particularly the RVLM, regulate sympathetic nerve activity. Centrally, Klo-neuropeptide reduces the impact of RVLM neurons on renal sympathetic nerve activity by stimulating Na^+/K^+-ATPase, thereby alleviating inflammatory gene expression (41). Activation of these neurons induces renal vasoconstriction, renin release, and tubular sodium and water reabsorption. Emerging evidence also suggested that hypertension may be an immune-mediated inflammatory disease (42). Animal studies showed that the sympathetic system interacts with the immune system, influencing inflammatory responses and contributing to fibrosis and disease progression (43). Recent research highlighted the crucial role of adrenoceptors in kidney disease. These receptors, found on sympathetic nerves, immune cells, and renal epithelial cells, mediate inflammatory and fibrotic responses when activated (44). Norepinephrine activates various adrenoceptors, contributing to chronic kidney disease by modulating physiological and pathophysiological effects. It also influences the immune system, increasing kidney infiltration and releasing inflammatory cytokines like *Tnfα*. As a result, the inhibition of renal sympathetic nerve activity has been demonstrated to reduce renal inflammation (45,46), suggesting a significant role of sympathetic signaling in mediating inflammation.

However, it has been suggested that Mec-sensitive nAChRs play a crucial role in regulating the expression of pro-inflammatory cytokines, such as the *Il1b* gene (47,48). This study focused on the α7nAChR, which selectively suppressed pro-inflammatory cytokines while sparing anti-inflammatory ones (49,50). To inhibit CAP, Mec, as an antagonist of nAChRs, was used. Generally, nicotinic receptor antagonists are preferred over muscarinic receptor antagonists for CAP modulation (51-53). Mec is considered a potential candidate for improving blood pressure and is also utilized as a drug with anti-addiction and anti-depressant properties. Also, the neuroprotective and anti-inflammatory effects of nicotine are counteracted by Mec. Therefore, it is plausible that some of the effects of Mec may be attributed to its impact on the CAP (54). Local inflammatory mediators, uremic toxins, or ischemic metabolites can elevate vagal nerve activity. Vagus nerve afferents play a central role in neuroimmune regulation during conditions like AKI, activating the CAP and suppressing systemic and local inflammation (55). The present study findings indicated that the parasympathetic system plays a crucial role in managing inflammation caused by AKI. Specifically, blocking the CAP system using Mec exacerbates peripheral inflammation.

Klo alone effectively reduced complications arising from IRI. Surprisingly, despite the inhibition of the CAP by Mec, Klo still exerted partial effects. This suggested that part of Klo central effects in the RVLM may be independent of the cholinergic system. These findings suggested that the sympathetic system

may be involved in this relationship. Given the impact of blood pressure and flow control on post-ischemic injuries (56), the current study proposed that Klo neuropeptide effects on the sympathetic system (4) are crucial for regulating peripheral effects (57).

CONCLUSION

In summary, this study demonstrated that AKI could trigger significant inflammatory responses. Klo alone, even with CAP system blockade, demonstrated positive effects, suggesting that Klo sympathetic control may be more significant than its parasympathetic contribution. Therefore, Klo, as a significant neuropeptide in the brain stem, may modulate kidney inflammation by influencing sympathetic nervous system function as well as alterations in immune system activity. Overall, the research underscored the impact of Klo and CAP inhibition on AKI-related outcomes, highlighting their roles in either alleviating or exacerbating renal injury or inflammation. To validate this hypothesis, further investigation is necessary. This study recommended evaluating Klo simultaneously with sympathetic system-blocking methods in the context of peripheral inflammation.

Acknowledgments

This research was financially supported by the Isfahan University of Medical Sciences, Isfahan, Iran (Grant No. 3400602).

Conflict of interest statement

The authors declared no conflict of interest in this study.

Authors' contributions

P. Reisi participated in designing the work, supervising the execution of the tests, analyzing the data, supervising the writing of the first draft of the manuscript and the writing of the final version; F. Ahmadi and E. Amohashemi performed the experiments, helped with data analysis, and wrote the first draft and final version of the manuscript. These investigators were aware of the treatment group allocation; H. Salehi participated in the histopathological examination; M. Kazemi executed real-time PCR; H. Salehi and M. Kazemi were unaware of the treatment group allocation. All authors read and approved the final version of the manuscript.

REFERENCES

1. Dolegowska K, Marchelek-Mysliwiec M, Nowosiad-Magda M, Slawinski M, Dolegowska B. FGF19 subfamily members: FGF19 and FGF21. J Physiol Biochem. 2019;75(2):229-240. DOI: 10.1007/s13105-019-00675-7.
2. Doi S, Zou Y, Togao O, Pastor JV, John GB, Wang L, *et al*. Klotho inhibits transforming growth factor-β1 (TGF-β1) signaling and suppresses renal fibrosis and cancer metastasis in mice. J Biol Chem. 2011;286(10):8655-8665. DOI: 10.1074/jbc.M110.174037.
3. Shin IS, Shin HK, Kim JC, Lee MY. Role of Klotho, an anti-aging protein, in pulmonary fibrosis. Arch Toxicol. 2015;89(5):785-795. DOI: 10.1007/s00204-014-1282-y.
4. Oshima N, Onimaru H, Yamagata A, Ito S, Imakiire T, Kumagai H. Rostral ventrolateral medulla neuron activity is suppressed by Klotho and stimulated by FGF23 in newborn Wistar rats. Auton Neurosci. 2020;224:102640,1-10. DOI: 10.1016/j.autneu.2020.102640.
5. Reisi P, Rashidi B, Arabpour Z, Shabrang M, Hamidi G. Effects of erythropoietin on neuronal apoptosis and neurogenesis in hippocampal dentate gyrus in the rat model of Alzheimer's disease. Res Pharm Sci. 2012;7(5):1026.
6. Luo K, Lim SW, Quan Y, Cui S, Shin YJ, Ko EJ, *et al*. Role of klotho in chronic calcineurin inhibitor nephropathy. Oxid Med Cell Longev. 2019;2019:1-7. DOI: 10.1155/2019/1825018.
7. Kuriyama N, Ozaki E, Mizuno T, Ihara M, Mizuno S, Koyama T, *et al*. Association between α-Klotho and deep white matter lesions in the brain: a pilot case-control study using brain MRI. J Alzheimer's Dis. 2018;61(1):145-155. DOI: 10.3233/JAD-170466.
8. Song J, Lee M, Kim Y, Park S, Kim J, Ryu S, *et al*. Developmental immunolocalization of the Klotho protein in mouse kidney epithelial cells. Eur J Histochem. 2014;58(1):19-26. DOI: 10.4081/ejh.2014.2256.
9. Zhu L, Stein LR, Kim D, Ho K, Yu GQ, Zhan L, *et al*. Klotho controls the brain-immune system interface in the choroid plexus. Proc Natl Acad Sci U S A. 2018;115(48):E11388-E11396. DOI: 10.1073/pnas.1808609115.
10. Hu MC, Shi M, Cho HJ, Zhang J, Pavlenco A, Liu S, *et al*. The erythropoietin receptor is a downstream effector of Klotho-induced cytoprotection. Kidney Int. 2013;84(3):468-481. DOI: 10.1038/ki.2013.149.
11. Haruna Y, Kashihara N, Satoh M, Tomita N, Namikoshi T, Sasaki T, *et al*. Amelioration of

progressive renal injury by genetic manipulation of Klotho gene. Proc Natl Acad Sci U S A. 2007;104(7):2331-2336.
DOI: 10.1073/pnas.0611079104.
12. Hu MC, Moe OW. Klotho as a potential biomarker and therapy for acute kidney injury. Nat Rev Nephrol. 2012;8(7):423-429.
DOI: 10.1038/nrneph.2012.92.
13. Hegde A, Denburg MR, Glenn DA. Acute kidney injury and pediatric bone health. Front pediatr. 2021;8:635628,1-7.
DOI: 10.3389/fped.2020.635628.
14. Hu MC, Kuro-o M, Moe OW. Klotho and kidney disease. J Nephrol. 2010;23(Suppl 16):S136-S144.
PMID: 21170871.
15. Hu MC, Kuro-o M, Moe OW. Klotho and chronic kidney disease. Contrib Nephrol. 2013;180:47-63.
DOI: 10.1159/000346778.
16. Chen L, Deng H, Cui H, Fang J, Zuo Z, Deng J, *et al*. Inflammatory responses and inflammation-associated diseases in organs. Oncotarget. 2018;9(6):7204-7218.
DOI: 10.18632/oncotarget.23208.
17. Rostami S, Emami-Aleagha MS, Ghasemi-Kasman M, Allameh A. Cross-talks between the kidneys and the central nervous system in multiple sclerosis. Caspian J Intern Med. 2018;9(3):206-219.
DOI: 10.22088/cjim.9.3.206.
18. de Jonge WJ, Ulloa L. The alpha7 nicotinic acetylcholine receptor as a pharmacological target for inflammation. Br J Pharmacol. 2007;151(7):915-929.
DOI: 10.1038/sj.bjp.0707264.
19. Kumagai H, Oshima N, Matsuura T, Iigaya K, Imai M, Onimaru H, *et al*. Importance of rostral ventrolateral medulla neurons in determining efferent sympathetic nerve activity and blood pressure. Hypertens Res. 2012;35(2):132-141.
DOI: 10.1038/hr.2011.208.
20. Zhang ZH, Wei SG, Francis J, Felder RB. Cardiovascular and renal sympathetic activation by blood-borne TNF-α in rat: the role of central prostaglandins. Am J Physiol Regul Integr Comp Physiol. 2003;284(4):R916-R927.
DOI: 10.1152/ajpregu.00406.2002.
21. Guyenet PG, Stornetta RL, Holloway BB, Souza GM, Abbott SB. Rostral ventrolateral medulla and hypertension. Hypertens. 2018;72(3):559-566.
DOI: 10.1161/HYPERTENSIONAHA.118.10921.
22. Barta P, Monti J, Maass PG, Gorzelniak K, Müller DN, Dechend R, *et al*. A gene expression analysis in rat kidney following high and low salt intake. J Hypertens. 2002;20(6):1115-1120.
DOI: 10.1097/00004872-200206000-00022.
23. Amohashemi E, Alaei H, Reisi P. Effects of GABAB receptor blockade on lateral habenula glutamatergic neuron activity following morphine injection in the rat: an electrophysiological study. Res Pharm Sci. 2023;18(1):16-23.
DOI: 10.4103/1735-5362.363592.
24. Jokar Z, Khatamsaz S, Alaei H, Shariati M. The electrical stimulation of the central nucleus of the amygdala in combination with dopamine receptor antagonist reduces the acquisition phase of morphine-induced conditioned place preference in male rats. Res Pharm Sci. 2023;18(4):430-438.
DOI: 10.4103/1735-5362.378089.
25. Sumitra M, Manikandan P, Rao KVK, Nayeem M, Manohar BM, Puvanakrishnan R. Cardiorespiratory effects of diazepam-ketamine, xylazine-ketamine and thiopentone anesthesia in male Wistar rats-a comparative analysis. Life Sci. 2004;75(15):1887-1896.
DOI: 10.1016/j.lfs.2004.05.009.
26. Aboul-Fotouh S. Behavioral effects of nicotinic antagonist mecamylamine in a rat model of depression: prefrontal cortex level of BDNF protein and monoaminergic neurotransmitters. Psychopharmacology. 2015;232(6):1095-1105.
DOI: 10.1007/s00213-014-3745-5.
27. Golab F, Kadkhodaee M, Zahmatkesh M, Hedayati M, Arab H, Schuster R, *et al*. Ischemic and non-ischemic acute kidney injury causes hepatic damage. Kidney Int. 2009;75(8):783-792.
DOI: 10.1038/ki.2008.683.
28. Paxinos G, Watson C. The rat brain in stereotaxic coordinates. 6th ed. Elsevier; 2006. pp. 136-137.
29. Landry T, Laing BT, Li P, Bunner W, Rao Z, Prete A, *et al*. Central α-Klotho suppresses NPY/AgRP neuron activity and regulates metabolism in mice. Diabetes. 2020;69(7):1368-1381.
DOI: 10.2337/db19-0941.
30. Chen LJ, Cheng MF, Ku PM, Lin JW. Rosiglitazone increases cerebral klotho expression to reverse baroreflex in type 1-like diabetic rats. Biomed Res Int. 2014;2014:309151,1-9.
DOI: 10.1155/2014/309151.
31. Oshima N, Onimaru H, Yamagata A, Ito S, Imakiire T, Kumagai H. Rostral ventrolateral medulla neuron activity is suppressed by Klotho and stimulated by FGF23 in newborn Wistar rats. Auton Neurosci. 2020;224:102640,1-10.
DOI: 10.1016/j.autneu.2020.102640.
32. Baluchnejadmojarad T, Eftekhari SM, Jamali-Raeufy N, Haghani S, Zeinali H, Roghani M. The anti-aging protein klotho alleviates injury of nigrostriatal dopaminergic pathway in 6-hydroxydopamine rat model of Parkinson's disease: involvement of PKA/CaMKII/CREB signaling. Exp Gerontol. 2017;100:70-76.
DOI: 10.1016/j.exger.2017.10.023.
33. Landry T, Li P, Shookster D, Jiang Z, Li H, Laing BT, *et al*. Centrally circulating α-klotho inversely correlates with human obesity and modulates arcuate cell populations in mice. Mol Metab. 2021;44:101136,1-15.
DOI: 10.1016/j.molmet.2020.101136.
34. Livak KJ, Schmittgen TD. Analysis of relative gene expression data using real-time quantitative PCR and the 2-ΔΔCT method. Methods. 2001;25(4):402-408.
DOI: 10.1006/meth.2001.1262.
35. Andrade L, Rodrigues CE, Gomes SA, Noronha IL. Acute kidney injury as a condition of renal senescence. Cell Transplant. 2018;27(5):739-753.
DOI: 10.1177/0963689717743512.

36. Wang Q, Su W, Shen Z, Wang R. Correlation between soluble α-Klotho and renal function in patients with chronic kidney disease: a review and meta-analysis. Biomed Res Int. 2018;2018:1-12. DOI: 10.1155/2018/9481475.
37. Maeda A, Hayase N, Doi K. Acute kidney injury induces innate immune response and neutrophil activation in the lung. Front Med. 2020;7:565010,1-5. DOI: 10.3389/fmed.2020.565010.
38. Reisi P, Eidelkhani N, Rafiee L, Kazemi M, Radahmadi M, Alaei H. Effects of doxepin on gene expressions of Bcl-2 family, TNF-α, MAP kinase 14, and Akt1 in the hippocampus of rats exposed to stress. Res Pharm Sci. 2017;12(1):15-20. DOI: 10.4103/1735-5362.199042.
39. Junaid A, Rosenberg M, Hostetter T. Interaction of angiotensin II and TGF-beta 1 in the rat remnant kidney. J Am Soc Nephrol. 1997;8(11):1732-1738. DOI: 10.1681/ASN.V8111732.
40. Dhingra S, Sharma AK, Arora RC, Slezak J, Singal PK. IL-10 attenuates TNF-α-induced NFκB pathway activation and cardiomyocyte apoptosis. Cardiovasc Res. 2009;82(1):59-66. DOI: 10.1093/cvr/cvp040.
41. Sopjani M, Alesutan I, Dërmaku-Sopjani M, Gu S, Zelenak C, Munoz C, *et al*. Regulation of the Na+/K+ ATPase by klotho. FEBS Lett. 2011;585(12):1759-1764. DOI: 10.1016/j.febslet.2011.05.021
42. Hering L, Rahman M, Potthoff SA, Rump LC, Stegbauer J. Role of α2-adrenoceptors in hypertension: focus on renal sympathetic neurotransmitter release, inflammation, and sodium homeostasis. Front Physiol. 2020;11:566871,1-11. DOI: 10.3389/fphys.2020.566871.
43. Carnevale D, Perrotta M, Pallante F, Fardella V, Iacobucci R, Fardella S, *et al*. A cholinergic-sympathetic pathway primes immunity in hypertension and mediates brain-to-spleen communication. Nat Commun. 2016;7(1): 13035,1-13. DOI: 10.1038/ncomms13035.
44. Hering L, Rahman M, Hoch H, Markó L, Yang G, Reil A, *et al*. α2A-adrenoceptors modulate renal sympathetic neurotransmission and protect against hypertensive kidney disease. J Am Soc Nephrol. 2020;31(4):783-798. DOI: 10.1681/ASN.2019060599.
45. Kamat NV, Thabet SR, Xiao L, Saleh MA, Kirabo A, Madhur MS, *et al*. Renal transporter activation during angiotensin-II hypertension is blunted in interferon-γ−/− and interleukin-17A−/− mice. Hypertension. 2015;65(3):569-576. DOI: 10.1161/HYPERTENSIONAHA.114.04975.
46. Wu J, Saleh MA, Kirabo A, Itani HA, Montaniel KRC, Xiao L, *et al*. Immune activation caused by vascular oxidation promotes fibrosis and hypertension. J Clin Invest. 2016;126(1):50-67. DOI: 10.1172/JCI80761.
47. Chernyavsky AI, Arredondo J, Skok M, Grando SA. Auto/paracrine control of inflammatory cytokines by acetylcholine in macrophage-like U937 cells through nicotinic receptors. Int Immunopharmacol. 2010;10(3):308-315. DOI: 10.1016/j.intimp.2009.12.001.
48. Piovesana R, Salazar Intriago MS, Dini L, Tata AM. Cholinergic modulation of neuroinflammation: focus on α7 nicotinic receptor. Int J Mol Sci. 2021;22(9):4912,1-12. DOI: 10.3390/ijms22094912.
49. Bonaz B, Sinniger V, Pellissier S. Targeting the cholinergic anti-inflammatory pathway with vagus nerve stimulation in patients with Covid-19? Bioelectron Med. 2020;6(1):15,1-7. DOI: 10.1186/s42234-020-00051-7.
50. Keever KR, Cui K, Casteel JL, Singh S, Hoover DB, Williams DL, *et al*. Cholinergic signaling via the α7 nicotinic acetylcholine receptor regulates the migration of monocyte-derived macrophages during acute inflammation. J Neuroinflammation. 2024;21(1):3,1-17. DOI: 10.1186/s12974-023-03001-7.
51. Báez-Pagán CA, Delgado-Vélez M, Lasalde-Dominicci JA. Activation of the macrophage α7 nicotinic acetylcholine receptor and control of inflammation. J Neuroimmune Pharmacol. 2015;10(3):468-476. DOI: 10.1007/s11481-015-9601-5.
52. Liu H, Zhang X, Shi P, Yuan J, Jia Q, Pi C, *et al*. α7 Nicotinic acetylcholine receptor: a key receptor in the cholinergic anti-inflammatory pathway exerting an antidepressant effect. J Neuroinflammation. 2023;20(1):84,1-19. DOI: 10.1186/s12974-023-02768-z.
53. Lv J, Ji X, Li Z, Hao H. The role of the cholinergic anti-inflammatory pathway in autoimmune rheumatic diseases. Scand J Immunol. 2021;94(4):e13092, 1-12. DOI: 10.1111/sji.13092.
54. Halder N, Lal G. Cholinergic system and its therapeutic importance in inflammation and autoimmunity. Front Immunol. 2021;12: 660342,1-29. DOI: 10.3389/fimmu.2021.660342.
55. Inoue T, Abe C, Kohro T, Tanaka S, Huang L, Yao J, *et al*. Non-canonical cholinergic anti-inflammatory pathway-mediated activation of peritoneal macrophages induces Hes1 and blocks ischemia/reperfusion injury in the kidney. Kidney Int. 2019;95(3):563-576. DOI: 10.1016/j.kint.2018.09.020.
56. Guyenet PG. The sympathetic control of blood pressure. Nat Rev Neurosci. 2006;7(5):335-346. DOI: 10.1038/nrn1902.
57. Kanbay M, Demiray A, Afsar B, Covic A, Tapoi L, Ureche C, *et al*. Role of Klotho in the development of essential hypertension. Hypertension. 2021;77(3):740-750. DOI: 10.1161/HYPERTENSIONAHA.120.16635.